HHS Public Access

Author manuscript

Cytotherapy. Author manuscript; available in PMC 2015 March 26.

Published in final edited form as:

Cytotherapy. 2014 January ; 16(1): 41–55. doi:10.1016/j.jcyt.2013.08.010.

Amniotic fluid stem cells prevent β-cell injury

VALENTINA VILLANI[1], **ANNA MILANESI**[2], **SARGIS SEDRAKYAN**[1], **STEFANO DA SACCO**[1], **SUSANNE ANGELOW**[1], **MARIA TERESA CONCONI**[3], **ROSA DI LIDDO**[3], **ROGER DE FILIPPO**[1], and **LAURA PERIN**[1]

[1]Department of Urology, Children's Hospital Los Angeles, University of Southern California, Los Angeles, California

[2]Division of Endocrinology, VA Greater Los Angeles Healthcare System, University of California Los Angeles, Los Angeles, California

[3]Department of Pharmaceutical Sciences, University of Padua, Padua, Italy

Abstract

Background aims—The contribution of amniotic fluid stem cells (AFSC) to tissue protection and regeneration in models of acute and chronic kidney injuries and lung failure has been shown in recent years. In the present study, we used a chemically induced mouse model of type 1 diabetes to determine whether AFSC could play a role in modulating β-cell injury and restoring β-cell function.

Methods—Streptozotocin-induced diabetic mice were given intracardial injection of AFSC; morphological and physiological parameters and gene expression profile for the insulin pathway were evaluated after cell transplantation.

Results—AFSC injection resulted in protection from β-cell damage and increased β-cell regeneration in a subset of mice as indicated by glucose and insulin levels, increased islet mass and preservation of islet structure. Moreover, β-cell preservation/regeneration correlated with activation of the insulin receptor/*Pi3K*/*Akt* signaling pathway and vascular endothelial growth factor-A expression involved in maintaining β-cell mass and function.

Conclusions—Our results suggest a therapeutic role for AFSC in preserving and promoting endogenous β-cell functionality and proliferation. The protective role of AFSC is evident when stem cell transplantation is performed before severe hyperglycemia occurs, which suggests the importance of early intervention. The present study demonstrates the possible benefits of the application of a non–genetically engineered stem cell population derived from amniotic fluid for the treatment of type 1 diabetes mellitus and gives new insight on the mechanism by which the beneficial effect is achieved.

Correspondence: **Laura Perin**, PhD, Department of Urology, Children's Hospital Los Angeles, 4661 Sunset Boulevard, Mailstop 35, Los Angeles, CA 90027. lperin@chla.usc.edu.

Disclosure of interests: The authors have no commercial, proprietary, or financial interest in the products or companies described in this article.

Supplementary data

Supplementary data related to this article can be found online at http://dx.doi.org/10.1016/j.jcyt.2013.08.010

Keywords

amniotic fluid; β-cell; pancreas; regeneration; stem cells; type 1 diabetes mellitus

Introduction

Diabetes mellitus has now reached epidemic proportions and represents a major health concern. Both type 1 and type 2 diabetes ultimately result in a significant loss of β-cell number and function. The disadvantages of current therapies such as exogenous insulin administration and islet or whole-organ transplantation solicit the urgency to find alternative approaches for the treatment of patients with insulin-dependent diabetes. A great deal of attention has recently been focused in the area of stem cell technology as a new, promising approach for the treatment of a variety of diseases. Several attempts to apply stem cells of various origin to treat diabetes mellitus have been documented in the past decade in both animal models and human clinical trials (1–11), but the question about how stem cells participate to tissue recovery is still open: either stem cells directly replace the injured tissue by transdifferentiation to the specific functional cell type, or stem cells exert their beneficial effect by protecting and stimulating endogenous regeneration.

Stem cells from different sources have been shown to be able to differentiate *in vitro* to insulin-producing cells on manipulation of culture conditions or cell transfection with key regulatory factors (12–15), but the same scenario has been demonstrated rarely in vivo in animal models of insulin-dependent diabetes (2,16–18).

Amniotic fluid–derived stem cells (AFSC) have emerged in recent years as a new source of pluripotent stem cells with immunological properties (19). In our laboratory, we have shown that AFSC present beneficial effects on models of kidney and lung diseases by restoring morphology and physiology of the damaged tissue (19–23). In these models, protection was achieved mainly by immunomodulation through paracrine action rather than differentiation of AFSC into kidney- or lung-specific cells. Recently, AFSC were induced to differentiate to insulin-producing cells by *Pdx1* transfection and controlled *in vitro* culture conditions (24), but there is no evidence for their application in *in vivo* diabetic models thus far. This study shows the *in vivo* therapeutic potential of AFSC for the treatment of insulin-dependent diabetes mellitus. AFSC prevented β-cell loss and damage and stimulated endogenous β-cell regeneration after pancreatic injury through activation of the Pi3Kinase/Akt pathway and vascular endothelial growth factor-A (VEGF-A) expression. Our study reports the first strong evidence that AFSC can potentially be used as tool to understand β-cell regeneration and offer an attractive therapeutic option for patients with insulin-dependent diabetes. Moreover, the advantage of AFSC application without preliminary genetic manipulation makes them a suitable candidate for the translation of cell therapy to the clinic.

Methods

Isolation, culture and preparation of human amniotic fluid stem cells and human fibroblast cell line

Under Institutional Review Board approval of Children's Hospital Los Angeles, human amniotic fluid samples with normal karyotype and normal fetal ultrasound images were collected from discarded amniocentesis between 15–20 weeks of gestation (kindly donated by Dr R. Habibian; Labcorp, Monrovia, CA, USA).

Expansion and isolation of stem cells is well established in our laboratory (19–23). Briefly, a selected c-*kit*-clone population was cultured and expanded in Petri dishes with the use of Chang's medium containing α-minimum essential medium supplemented with 20% Chang B, 2% Chang C (Irvine Scientific, Santa Ana, CA, USA), L-glutamine, 20% of ES–fetal bovine serum and 1% of Pen/Strep antibiotic solution (Gibco/Invitrogen, Life Technologies, Carlsbad, CA, USA). AFSC were expanded for 40 passages and cultured under humidified conditions at 37°C and 5% CO_2 and trypsinized with 0.25% trypsin–ethylenediaminetetra-acetic acid.

To track the injected cells, AFSC were labeled with the cell tracker CM-DiI (Molecular Probes, Life Technologies, Carlsbad, CA, USA), following the manufacturer's instructions. Briefly, cell suspension was incubated with a working solution of 0.04 mg/ mL of CM-DiI and incubated for 5 min at 37°C and then 15 min at 4°C. Cells were finally washed three times in phosphate-buffered saline (PBS) (Gibco/ Invitrogen, Life Technologies).

Human lung fibroblasts (negative control) were purchased from LifeLine Cell Technology (Carlsbad, CA, USA). Fibroblast cells were expanded with Fibrolife Media (LifeLine Cell Technology) on tissue culture dishes for up to five passages. At the moment of injection, fibroblasts were prepared as previously described for AFSC.

Animal model and stem cell transplantation

Immunodeficient NOD/SCID (NOD.CB17-Prkdc^{scid}/J) mice were purchased from the Jackson Laboratory (Sacramento, CA, USA). All the procedures described and animal protocols were approved by the Institutional Animal Care and Use Committee (IACUC) at Children's Hospital Los Angeles. To induce diabetes, 8-week-old male NOD/ SCID mice were treated with the use of a protocol of multiple low-dose injections of streptozotocin (STZ). Briefly, mice were given STZ [2-Deoxy-2-(3-methyl 1-3-nitrosoureido)-D-glucopyranose, Sigma-Aldrich, Saint Louis, MO, USA], 50 mg/kg body wt, by intraperitoneal injection, for 3 consecutive days. Mice were fasted 4 h before each injection; STZ was dissolved in 50 mmol/L sodium citrate buffer, pH 4.5, and injected into mice within 5 min of preparation. On experimental day 4, 1 day after completion of STZ treatment, mice received cell injections of either 1×10^6 AFSC or fibroblasts and saline solution. Cells and saline solution were administered by intracardiac injection through the chest wall into the left ventricle with the use of a 29-gauge needle. Mice were carefully monitored under isofluorane inhalation anesthesia. Two cell injections were performed independently to test long-term (4 weeks) and short-term (72 h) response of mice after transplantation.

The experimental groups (for a total of 63 mice) were divided as follows: Group 1: STZ-treated mice to determine the disease model (n = 13)

Group 2: Mice receiving AFSC after STZ treatment (n = 10 for 72-h time point, n = 9 for 4-week time point)

Group 3: Mice receiving fibroblast after STZ treatment (n = 5 for 72-h time point, n = 7 for 4-week time point)

Group 4: Mice receiving saline solution after STZ treatment (n = 5 for 72-h time point, n = 6 for 4-week time point)

Group 5: Healthy control mice not receiving any treatment (n = 8)

Mice were euthanized by CO_2 inhalation for tissue harvesting and subsequent analysis at 72 h and 4 weeks after cell transplantation.

In addition, to evaluate the effects of AFSC injection once hyperglycemia was established (600 mg/dL), a total of 11 mice (n = 3 mice injected with AFSC after STZ treatment; n = 4 mice treated with STZ; n = 4 mice health control mice) were used. The mice were injected at 14 days after STZ treatment and euthanized at 5 weeks after cell injections.

Blood glucose and plasma insulin measurements

Mice from all experimental groups were monitored for blood glucose level every 2 days for the first week after treatment and then once per week for the 4-week experiment. All measurements were performed after 5-h fasting. Blood glucose was measured from the tail vein with the use of the OneTouch UltraMini Blood Glucose Monitoring System (Lifescan, Milpitas, CA, USA). The sensitivity of the system does not exceed 600 mg/dL; thus, in some cases, the extent of hyperglycemia was over the limit of the sensitivity of the instrument.

Plasma insulin levels were determined by mouse enzyme-linked immunosorbent assay (Mercodia, Winston-Salem, NC, USA), according to manufacturer's instructions. Whole blood was withdrawn from the facial vein, and plasma was separated by centrifugation at 14,000 rpm for 3 min in plasma separator tubes with lithium heparin (BD, Franklin Lakes, NJ, USA). Briefly, 10 μL of plasma samples and calibrators were aliquoted in a mouse monoclonal anti-insulin antibody-coated 96-well plate. Working solution containing peroxidase-conjugated anti-insulin antibody was then added to each well (100 μL per well), and the plate was put under shaking conditions at room temperature (RT) for 2 h. After six washes with washing buffer, 200 μL of 3,3′,5,5′-tetramethylbenzidine substrate was added to each well and allowed to incubate for 15 min at RT. The reaction was stopped with 0.5 mol/L H_2SO_4, and optical density (OD) read at 450 nm with the use of the Victor3 multilabel plate reader (PerkinElmer, Waltham, MA, USA). A standard curve was drawn by plotting OD_{450} and insulin concentration of calibrators with the use of Sigmaplot 11 data analysis software (Systat Software Inc, San Jose, CA, USA) and used as reference to extrapolate sample values for insulin concentrations.

Immunohistochemical analyses

Mouse pancreata were harvested at 72 h and 4 weeks for all the experimental groups and immediately processed for paraffin embedding. Tissues were fixed in 10% neutral phosphate buffer formalin (Polysciences Inc, Warrington, PA, USA) for 1 h at 4°C and stored in 70% ethanol overnight at 4°C. Tissues were subsequently dehydrated through graded ethanol, toluene and finally embedded in paraffin (TissuePrep, Fisher Scientific, Pittsburgh, PA, USA). Pancreatic sections (6 μm) were prepared with the use of a Leica RM2235 rotary microtome and deparaffinized in Histochoice clearing agent (Sigma-Aldrich) and rehydrated through graded ethanol series (100%, 90%, 70%, 50% and 30%) followed by rinsing in distilled water before use. For morphological evaluation, sections were stained in hematoxylin solution Gill N.3 (Sigma-Aldrich) and Eosin Y solution (Harleco, Millipore Corp, Billerica, MA, USA) (hematoxylin and eosin), rinsed in distilled water, dehydrated in ethanol and mounted with Xylene mounting medium (Fisher Scientific, Hampton, NH, USA). Stained sections were observed under a Leica DM1000 light microscope. For immunofluorescent staining, blocking was performed in a 2% bovine serum albumin (Jackson Immunoresearch Laboratories Inc, West Grove, PA, USA) solution in PBS × 1 before incubation for 1 h at RT with the following primary antibodies: anti-insulin/proinsulin mouse monoclonal antibody (dilution 1:500); anti-glucagon rabbit polyclonal antibody (dilution 1:50). After PBS washing, sections were incubated for 30 min at RT with secondary antibodies, respectively, Alexa fluor 555 donkey anti-mouse immunoglobulin (Ig)G and Alexa fluor 488 donkey anti-rabbit IgG, dilution 1:400. Sections were mounted with Vectashield mounting medium with 4′,6-diamidino-2-phenylindole (Vector Laboratories, Burlingame, CA, USA). Images were captured with the use of a Leica AF6000 fluorescent microscope. Proliferating cell nuclear antigen (PCNA) and VEGF-A antigen protein expression was detected by immunoperoxidase staining. Briefly, sections were blocked with 3% H_2O_2 in methanol for 10 min at RT to mask endogenous peroxidases. After heat-mediated antigen retrieval with antigen unmasking solution (H-3300, Vector Laboratories) was performed, samples were incubated with 2% bovine serum albumin blocking solution for 30 min at RT. Primary rabbit polyclonal anti-PCNA antibody, dilution 1:1000, and rabbit polyclonal anti–VEGF-A antibody, dilution 1:100, were used for incubation for 1 h at RT. Signal detection was obtained by incubation with the ImmPRESS universal antibody (anti-mouse IgG/anti-rabbit IgG, peroxidase) detection kit for 30 min at RT followed by incubation with ImmPACT 3,3′-diaminobenzidine peroxidase substrate, both purchased from Vector Laboratories. Slides were finally rinsed, dehydrated in 90% and 100% ethanol (5 min each) and mounted with Protocol mounting medium xylene (Fisher Scientific, Hampton, NH, USA). Images were captured with the use of a Leica DM1000 light microscope. All primary antibodies were purchased from Abcam (Cambridge, MA, USA). All secondary Alexa fluorochrome-conjugated antibodies were purchased from Life Technologies.

Quantification of islet mass, β-cell/α-cells and proliferating cells

Pancreatic tissues from all the experimental groups were processed, and histological samples were prepared as previously described. Serial sections were cut at a distance of 100 μm, and 10 different islets were considered per mouse for the counting. For each experimental group, at least three mice were included. Slides were stained with hematoxylin and eosin for islet

mass quantification and immunostained to detect insulin/glucagon/PCNA-positive cells as previously reported. Islet mass is expressed as total number of counted cells in 10 islets per mouse. Hormone-expressing cells and proliferating cells were quantified as percentage of marker-positive cells over the total nuclei counted per islet (10 islets per mouse).

Real-time polymerase chain reaction arrays

On euthanasia of the mice, 4 weeks after cell injection, pancreatic tissue from all the experimental groups was removed and stored in RNAlater (Qiagen, Valencia, CA, USA) until further processing. RNA was extracted from the whole tissue by column method with the use of the RNeasy Mini kit (Qiagen) according to the manufacturer's instructions and quantified with the use of the Nanodrop system (Thermo Scientific, Waltham, MA, USA). Complement DNA was obtained from the extracted RNA by retrotranscription with the RT2 First Strand Kit (SABiosciences, Qiagen), according to the manufacturer's instructions. The complement DNA of each sample was then added to the RT2 SYBR Green qPCR Master Mix and aliquoted for gene expression analysis on specific arrays for the insulin-signaling pathway (PAMM-030; SABiosciences). Gene analysis including significant values and fold changes was performed with the online tool provided by SABiosciences (http://www.sabiosciences.com/pcrarraydataanalysis.php).

Statistical analysis

Statistical analysis was performed with the use of SigmaPlot 11 data analysis software (Systat Software Inc). All data are presented as mean ± standard error of the mean. For comparison of multiple groups, we used one-way analysis of variance followed by the Newman-Keuls test for data sets that passed the Shapiro-Wilk normality test or Mann-Whitney rank-sum test/Dunn's method for data that failed the Shapiro-Wilk normality test. A value of $P < 0.05$ was considered as statistically significant of the test results.

Results

Establishment of the disease model and physiological response to AFSC treatment

Treatment of mice with the diabetogenic drug STZ for 3 consecutive days resulted in the development of significant hyperglycemia by experimental day 8, when the average blood glucose reached a value near 400 mg/dL (Figure 1A). We confirmed that all STZ-treated mice (n = 13) reached a significant level of hyperglycemia of 600 mg/dL or above, which remained consistent for the duration of the experiment and never returned to normal. Thus, we could establish with confidence, in our laboratory and under the condition used, that the STZ in NOD/SCID mice was a reproducible model for our experiments. Mice were divided into two groups, one receiving the STZ dose and one healthy control group as reference. Blood glucose values of STZ-treated mice remained significantly higher compared with healthy control mice for up to 4 weeks (Figure 1A). Disease establishment was confirmed morphologically by histochemical analysis. Strong reduction of islet mass was detected by hematoxylin and eosin staining in STZ-treated mice compared with control mice 4 weeks after drug treatment (Figure 1B,C). The histological data were confirmed by direct quantification of the islet mass in healthy control mice and in STZ-treated mice (Figure 1D).

Subsequently, on experimental day 4, STZ-treated mice were transplanted with 1×10^6 of either AFSC or human fibroblasts or injected with saline vehicle. AFSC-injected mice (n = 4) were able to maintain normal blood glucose values at 4 weeks after cell injection, significantly lower compared with diabetic STZ-treated mice (defined as responsive mice). A group of AFSC-injected mice (n = 5) showed a disease progression comparable to STZ-treated control mice (defined as non-responsive mice). Fibroblast (n = 7) and saline (n = 6) injections did not prevent development of permanent hyperglycemia with a value of glucose >400 mg/dL (Figure 1E).

At 4 weeks from stem cell transplantation, plasma insulin level was significantly higher in AFSC-responsive mice compared with the other treatment groups, which all had significantly lower amounts of circulating insulin than did the healthy control mice (Figure 1F).

Preservation of islet mass, insulin and glucagon expression 4 weeks after AFSC treatment

Histological examination at 4 weeks after transplantation (Figure 2A–L) showed severe alteration of the pancreatic islet morphology and significant reduction of the number of insulin-expressing cells in the STZ-induced diabetic mice (Figure 2C,D), AFSC–non-responsive mice (Figure 2G,H), fibroblast-injected mice (Figure 2I,J) and saline-injected mice (Figure 2K,L). In contrast, the morphology of pancreatic islets was maintained, and the staining pattern of insulin and glucagon in the pancreatic islets of AFSC-responsive mice (Figure 2E,F) was very similar to that of the healthy control mice (Figure 2A,B). AFSC-responsive mice presented a total islet mass significantly higher than that in STZ-treated mice and other treatment groups at 4 weeks after cell injection (Figure 2M). As expected, STZ treatment resulted in a drastic reduction of insulin-expressing β-cells compared with that in healthy control mice (Figure 2N). In contrast, AFSC-responsive mice showed a significantly higher β-cell number than did STZ-treated, AFSC–non-responsive and fibroblast-injected and saline injected mice (Figure 2N). Moreover, we observed a significant increase in proportion of glucagon-expressing α-cells in the pancreatic islets of all treatment groups compared with that in healthy control mice (Figure 2O). All injected mice, however, presented a significantly lesser increase of α-cells in respect to the STZ-treated diabetic mice. Taken together, these results confirm preservation of the insulin-glucagon–expressing cell ratio and distribution only in the AFSC-responsive mice, as shown in Figure 2P. Further investigation did not show donor-labeled AFSC in the pancreas of transplanted mice 4 weeks after stem cell injection (data not shown). As already reported by our group, detection of injected cells was very rare at later time points (20,23), which suggests an early intervention of AFSC immediately after transplantation by either protection or activation of endogenous regeneration.

Level of blood glucose at the time of injection correlated with clinical response to AFSC treatment

To define the possible mechanism accountable for the difference in outcomes between responsive and non-responsive mice to AFSC transplantation, we hypothesized that early stem cell treatment could have a beneficial effect in the host tissue after injury. Our observations (Figure 3A) indicate that mice that showed a positive response to the AFSC

treatment (responsive mice) had blood glucose levels below a threshold that we defined on the basis of our experimental results at 200 mg/dL, at the time of stem cell injection.

Therefore, to confirm our hypothesis, we performed injections of AFSC at a later time point, specifically after 14 days after STZ treatment, when glucose level reached approximately 600 mg/dL. As demonstrated in a representative experiment (Figure 3B), the later time point injection of AFSC was not efficient for rescuing any hyperglycemic mice, thus supporting our hypothesis of beneficial early intervention.

We repeated cell injections in the experimental groups and analyzed the results 72 h after cell injection. We confirmed through this second group of injections that AFSC-responsive mice (n = 7) presented levels of blood glucose comparable to the healthy control mice and significantly lower than those of STZ-treated mice (n = 3). Conversely, injection of fibroblasts (n = 5) or saline vehicle (n = 5) when the blood glucose is below 200 mg/dL did not prevent the developing hyperglycemia at 72 h from the injection (Figure 3C). We also confirmed that all the mice responsive to AFSC treatment presented at the time of cell transplantation had blood glucose values below the defined threshold. There was not a statistically significant difference in the insulin levels in all mice at 72 h (Figure 3D), although AFSC were detectable in the host tissue at 72 h after transplantation. Despite the low amount that prevented accurate quantification, CM-Dil–labeled AFSC were found in exocrine tissue and, more interestingly, in endocrine tissue, as shown in Figure 3E,F.

Islet mass, insulin and glucagon expression 72 h after AFSC treatment

Immunohistochemical analysis (Figure 4A–J) of pancreata 72 h after AFSC treatment demonstrated the rapid beneficial effect of AFSC in terms of preservation of islet mass and hormone expression. AFSC-responsive mice showed preservation of islet mass (Figure 4E), together with the typical distribution of insulin and glucagon expression (Figure 4F), similar to that in the control mice (Figure 4A,B) and in contrast with that observed in STZ-treated mice (Figure 4C,D), fibroblast-injected mice (Figure 4G,H) and saline-injected mice (Figure 4I,J). Islet mass in AFSC-responsive mice was preserved, similar to that in the healthy control mice and significantly higher compared with the STZ-treated and other treatment groups (Figure 4K). Notably, there was a significant increase in islet mass of AFSC-responsive mice over time, from 72 h to 4 weeks after stem cell transplantation, which suggests not only protection of pancreatic islet cell mass from injury but also an increased islet cell proliferation (Figure 4L). The percentage of insulin-expressing cells in the mice responsive to AFSC treatment was similar to that in the healthy control mice and was significantly higher when compared with the other treatment groups (Figure 4M). Interestingly, pancreata from fibroblast- and saline-injected mice showed significantly lower insulin expression than that in STZ-treated mice. Although the glucagon-positive cells are not significantly different in all groups (Figure 4N), we observed preservation of the insulin:glucagon ratio in AFSC-responsive mice similar to that in the healthy control group and significantly higher than in the other treatment groups (Figure 4O).

AFSC-responsive mice displayed higher intra-islet proliferation and VEGF-A expression

To further examine the mechanism by which pancreatic islets are preserved after AFSC transplantation and to further support the previously described findings of increased islet mass over time from the early time point to 4 weeks after injection, we analyzed the level of cell proliferation within the islets of healthy mice, STZ-induced mice and the other treatment groups (Figure 5A,C,E,G,I). There was no difference in PCNA-positive cell number within the islets of healthy control mice and STZ-treated mice (Figure 5A,C,K). A slight increase was observed for the mice injected with both fibroblasts and saline, although it was not significant (Figure 5G,I,K). In contrast, a significant increase in the percentage of proliferating cells was observed within the islets of AFSC-responsive mice (Figure 5E,K). Analysis of the expression of VEGF-A by immunohistochemistry revealed stronger expression in the pancreatic islets of AFSC-responsive mice (Figure 5F) when compared with healthy control, STZ-treated, fibroblast-injected and saline-injected mice (Figure 5B,D,H,J).

Activation of the insulin receptor/Pi3K pathway mediated β-cell survival and proliferation in AFSC-responsive mice

To further investigate the mechanisms by which AFSC promote restoration of *β*-cell function in AFSC-responsive mice, we analyzed the level of expression of genes specifically involved in the insulin/receptor signaling pathway (Figure 6A–D). Insulin expression was significantly downregulated in STZ-treated mice, fibroblast-injected, saline-injected and AFSC–non-responsive mice and consistently higher in the pancreata of AFSC responsive mice (Figure 6A). Polymerase chain reaction (PCR) array results exhibited a general trend of decreased gene expression for the STZ-treated mice compared with control mice (Figure 6B). Genes encoding for proteins involved in the formation of the insulin receptor complex such as growth factor receptor–bound protein 10 (*Grb10*) and protein tyrosine phosphatase receptor type F (*Ptprf*) were significantly down-regulated in STZ-treated mice. In addition, STZ-treated mice demonstrated a significant decrease in the expression of genes involved in regulating glucose metabolism and glucose sensing, such as fructose bisphosphatase (*Fbp1*) and hexokinase 2 (*Hk2*), also targets of the phosphoinositol 3-kinase (*Pi3K*) pathway, and protein metabolism such as glycogen synthase kinase 3*β* (*Gsk3b*). In concordance, phosphatidylinositol 3-kinase regulatory subunit 1 (*Pik3r1*) and protein kinase c iota (*Prkci*), which are components of the Pi3K pathway, were significantly downregulated in STZ-treated mice, confirming the clear trend of decreased expression. The expression of *Rras2*, a critical *in vivo* regulator of the transforming growth factor-*β* signaling, was as well significantly reduced. Resistin (*Retn*), also known as adipose tissue–specific secretory factor showed upregulation, although not significantly.

Interestingly, pancreata from AFSC-responsive mice, compared with STZ-treated mice, (Figure 6C) showed significant increased expression of genes required for glucose metabolism such as glucokinase (*Gck*), phosphoenolpyruvate carboxykinase 2 (*Pck2*) and pyruvate kinase isozyme, liver and red blood cells (*Pklr*). Moreover, a significant upregulation of the serine/threonine kinase *Akt1*, also known as protein kinase B, a potent mediator of the *PI3K* signaling pathway, was detected in AFSC-responsive mice together with increased expression of the two isoforms *Akt2* and *Akt3*. *Akt2* in particular is involved

in the insulin pathway and is important for induction of glucose transport and regulation of glucose homeostasis (25). Consistently, phosphatidylinositol 3-kinase, regulatory subunit beta1 (*Pik3r1*) and beta2 (*Pik3r2*) and Prkci of *Pi3K* pathway machinery were increased. More interestingly, VEGF-A, a downstream target of the *Pi3K* signaling pathway, together with the above-mentioned *Hk2* and *Pck2*, were significantly upregulated in the AFSC-responsive mice. The panel of significantly upregulated genes also included Gsk3b, the serine/threonine protein kinase A-*raf* (*Araf*) that participates in the mitogen-activated protein kinase (*MAPK*) pathway, an important cascade regulating cell proliferation and differentiation and CCAAT/enhancer-binding protein-α (*Cebpa*), a transcription factor involved in protein metabolism. Gene expression analysis for the fibroblast-injected samples did not reveal any significant change for the previously described pathways compared with the STZ-treated group except for a slight upregulation of *Gsk3b*, whereas saline-injected mice showed significant upregulation only for Cebpa and the PI3K pathway component protein kinase Cγ (*Prkcc*). Noticeably, significant upregulation of some listed genes, including *Akt1*, *Araf*, *Cebpa*, *Fbp1*, *Grb10*, *Gsk3b*, *Pik3r2*, *Prkcc* and *Rras2*, was also detected in AFSC–non-responsive mice compared with STZ-treated mice, despite the physiological outcome (Figure 6C). Gene expression was also analyzed for all the injected groups in comparison to healthy control mice, as shown in Figure 6D and Supplementary Table I. The expression profile of AFSC-responsive mice was similar to that of healthy control mice, with the exception of a few significantly upregulated genes, such as the sterol regulatory element–binding transcription factor 1 (*Srebf1*), *Prkcc* and *VEGF-A* for the *Pi3K* pathway and *ras*-related protein (*Rras*), which was shown to have a role in blood vessel homeostasis (26). Both fibroblast-injected and saline-injected mice showed a general downregulation for most of the genes codifying proteins associated with the insulin receptor or involved in glucose metabolism and the PI3K pathway. In particular, *Grb10*, *Hk2*, *Pik3r1* and *Ptprf* were significantly downregulated. Significant upregulation was detected for *Prkcc* in saline-injected samples and *VEGF*-A for fibroblast-injected mice, although the increase was not substantial. Interestingly, resistin, whose upregulation was detected in STZ-treated mice compared with control mice, was strongly upregulated in fibroblast-injected and in AFSC–non-responsive mice (Figure 6D).

Discussion

Stem cell therapy has thus far been regarded as the most promising alternative treatment for insulin-dependent diabetes mellitus. Few studies have reported the ability of stem cells isolated from various sources to *in vitro* differentiate into insulin-like phenotype or to restore β-cell function *in vivo* (1–8,12–18). Different cell behaviors have been detected, depending on the type of stem cells and the animal model (2–6,16–18). Here we present the *in vivo* therapeutic potential of a recently discovered stem cell population, human AFSC, to preserve β-cell function by promoting endogenous regeneration in a chemically induced murine model of type 1 diabetes.

Our results indicate that AFSC, transplanted in STZ-induced diabetic mice, were able to protect β-cell function and preserve physiological parameters as indicated by euglycemia and normal plasma insulin levels 4 weeks after cell injection. Nearly half of the injected mice responded to AFSC treatment. Responsive mice showed preservation of islet mass and

morphology as well as insulin expression and secretion. We noticed that all mice rescued by AFSC treatment presented near-normal glycemic values (defined as glucose <200 mg/dL) at the time of stem cell injection; in fact, our data showed that AFSC prevented hyperglycemia and preserved pancreatic insulin secretion only if transplanted before the major injury has occurred. Our hypothesis is supported also by the evidence that if the cells are injected when severe hyperglycemia is present, mice do not recover. Thus, this observation suggests that not only the timing of injection plays a crucial role but that the degree of damage is important in determining the outcome. This mechanism of action by AFSC is also evident in our previous publications (19,20); in particular, we demonstrated that AFSC show renal protection in a model of acute tubular injury only if injected early before the acute phase of the damage.

An univocal mechanism by which stem cells may perpetrate their beneficial effect must be elucidated. Previous reports have shown very low and inconsistent *in vivo* differentiation of donor cells to insulin-producing cells, which supports the hypothesis of an endogenous regeneration by activation of endocrine progenitors or β-cell proliferation (2,18).

AFSC promoted their beneficial effect by protecting β-cells from injury and favoring endogenous β-cell proliferation, as indicated by increased proliferation rate within the islets of transplanted mice, which is responsible for the increase of pancreatic islet mass throughout the 4-week recovery period after cell injection. Despite the controversy surrounding the origin of newly derived β-cells, some evidence supports the conclusion that proliferation of differentiated β-cells is the predominant mechanism of regeneration (27,28). However, this is not to exclude that in different scenarios, other putative progenitors not yet fully identified might be activated (29–31). Considering the low amount of AFSC homing and the rapidity of the physiological response soon after cell transplantation, it is plausible to hypothesize that the beneficial potential relies on AFSC ability to promote survival and proliferation of preexisting β-cells rather than differentiating themselves to insulin-producing cells, because we did not detect AFSC differentiation within the pancreas at later time point. The contribution of exogenous stem cells to *in vivo* tissue regeneration through paracrine mechanisms, thus by signals promoting host cell proliferation or differentiation from endogenous precursors, has already been hypothesized in models of type 1 diabetes and acute cardiac injury and by our group on lung and kidney damage models (2,18,23,32).

The pancreas of AFSC-responsive mice showed upregulation of the insulin receptor/*Pi3K* pathway at the messenger RNA level. Activation of the *Pi3K* pathway by insulin interaction with its specific receptor has been hypothesized to define the beneficial outcome observed in diabetic mice responsive to AFSC. Several gene targets in the *Pi3K* cascade were upregulated, including *Akt1*, which is a well-known critical mediator of this pathway (33). *Akt* activity has been linked to processes promoting cell survival by inhibiting apoptosis and enhancing cell proliferation (34) and is a regulator of β-cell metabolism (35). Transgenic mice producing constitutively active Akt in the β-cells showed remarkable β-cell mass expansion through enhanced proliferation and reduced apoptosis (36). *Akt* is also known to be involved in pro-angiogenic mechanisms (37,38).

Interestingly, *Gsk3b* gene expression was also upregulated. *Gsk3b* is another downstream target of *Akt* and becomes inactivated by *Akt*-mediated phosphorylation on Ser9. Its activity has been correlated to degradation of β-catenin and it is usually considered a negative regulator of cell proliferation through inhibition of the Wnt/β-catenin pathway (39). Therefore, our data showing the increased expression of *Gsk3b* in the pancreas of AFSC-responsive mice compared with diabetic mice are an apparent contradiction. However, it has been reported recently that conditional ablation of *Gsk3b* in pancreatic β-cells resulted in expanded β-cell mass through increased proliferation, associated with enhanced signaling through the *Pi3k/Akt* pathway (40). This suggests that *Gsk3b* is rate-limiting for β-cell mass and controls β-cell growth as a mechanism of feedback inhibition on the insulin receptor/*Akt* pathway. On this view, *Gsk3b* is more a cell cycle regulator than a cell cycle repressor. *Gsk3b* has a key role of gatekeeper over a wide range of transcription factors and is fundamental for maintaining cells at a regulated rate of proliferation (41). Moreover, there is well-supported evidence that *Gsk3b* plays a role in modulating apoptosis and inhibits cell death, blocking the extrinsic apoptotic pathway (42). It is possible to speculate that the reduction of *Gsk3b* gene expression after STZ treatment reflected a deficiency in both cell cycle control and anti-apoptotic effect, and the significantly increased *Gsk3b* expression correlates with increased cell survival and reduced apoptosis, indicating the importance of *Gsk3b* in the maintenance of cell homeostasis. Cell proliferation is thus enhanced but in a controlled manner.

Interestingly, even if non-responsive mice show an increase of different genes involved in the insulin pathway in certain respects similar to the responsive mice (eg, *Gsk3b*), there was no evidence of pancreas protection at later time point; thus, it might be possible that higher levels of glycemia caused by STZ injury might have significantly damaged β-cells, unlikely to be reversible at that point by AFSC. Moreover, it is important to emphasize that fibroblasts do not show a significant change of insulin pathway signaling, thus confirming the specific activation of the pathway by AFSC.

In keeping with the observation of enhanced insulin receptor/*Pi3K*/*Akt* signaling, the pancreatic islets of AFSC-responsive mice showed a significantly increased expression of VEGF-A, both at the messenger RNA level and at the protein level. The strong interconnection occurring between β-cells and the endothelium is documented. The importance of VEGF-A as a factor stimulating intra-islet vascularization, which is a necessary condition for β-cell survival, proliferation and functionality, has been reported (43). The release of VEGF-A is meant to attract endothelial cells through interaction with the specific receptor VEGFr-2 and consequent formation of a vascular basement membrane that represents a niche for insulin gene expression and β-cell proliferation (44). The highly increased VEGF-A expression in the pancreatic islets of AFSC-responsive mice might indicate an increase of intra-islet angiogenesis that could contribute to preservation of β-cell function and β-cell regeneration. Notably, transgenic expression of VEGF-A in isolated human islets and murine pancreatic islets was shown to drive an increase of β-cell mass and function by enhancing angiogenesis (45).

Mice responsive to AFSC showed an overall tendency to upregulation of genes involved in the cell cycle. Significantly, an increase of gene expression was in fact observed for *Araf*, a

serine/threonine kinase of the *Raf* kinase family, which participates in the *MAPK* signaling cascade, as well linked to boosting of cell proliferation and differentiation (46). Moreover, significant upregulation of Rras was detected for AFSC responsive mice compared with healthy control mice. *Rras* is a regulator of cell survival and important for vascular homeostasis (26). We recently reported that human bone marrow mesenchymal stromal cells, genetically engineered to overexpress VEGF-A, were able to reverse hyperglycemia in an STZ-induced diabetic mouse model mainly by induction of endogenous β-cell regeneration through activation of the insulin/*Igf1* receptor/*Pi3K*/*Akt* pathway and increased VEGF-A expression (8). We not only confirm a potentially very important mechanism in β-cell regeneration/protection after injury, but we show for the first time that AFSC are able to promote endogenous β-cell proliferation by stimulating the *Pi3K* pathway and enhancing VEGF-A expression.

The present findings confirm the potential of AFSC for the treatment of insulin-dependent diabetes mellitus mainly through modification of *in situ* milieu, with consequent protection and stimulation of endogenous β-cell regeneration to sustain full functional restoration. In conclusion, our work is the first evidence of the possible important therapeutic use of a new and promising stem cell source for insulin-dependent diabetes and represents a new model to study β-cell recovery after injury.

Supplementary Material

Refer to Web version on PubMed Central for supplementary material.

Acknowledgments

We thank Fondazione Ing Aldo Gini (University of Padua) for funding support to the present research. We also would like to thank Dr Habibian for providing the human amniotic fluid samples. This work was supported by The Iacocca foundation and GOFARR.

References

1. Soria B, Roche E, Berná G, León-Quinto T, Reig JA, Martín F. Insulin-secreting cells derived from embryonic stem cells normalize glycemia in streptozotocin-induced diabetic mice. Diabetes. 2000; 49:157–62. [PubMed: 10868930]
2. Hess D, Li L, Martin M, Sakano S, Hill D, Strutt B, et al. Bone marrow-derived stem cells initiate pancreatic regeneration. Nat Biotechnol. 2003; 21:763–70. [PubMed: 12819790]
3. Lee RH, Seo MJ, Reger RL, Spees JL, Pulin AA, Olson SD, et al. Multipotent stromal cells from human marrow home to and promote repair of pancreatic islets and renal glomeruli in diabetic NOD/SCID mice. Proc Natl Acad Sci U S A. 2006; 103:17438–43. [PubMed: 17088535]
4. Naujok O, Francini F, Picton S, Bailey CJ, Lenzen S, Jörns A. Changes in gene expression and morphology of mouse embryonic stem cells on differentiation into insulin-producing cells in vitro and in vivo. Diabetes Metab Res Rev. 2009; 25:464–76. [PubMed: 19425055]
5. Jurewicz M, Yang S, Augello A, Godwin JG, Moore RF, Azzi J, et al. Congenic mesenchymal stem cell therapy reverses hyperglycemia in experimental type 1 diabetes. Diabetes. 2010; 59:3139–47. [PubMed: 20841611]
6. Raikwar SP, Zavazava N. Spontaneous in vivo differentiation of embryonic stem cell-derived pancreatic endoderm-like cells corrects hyperglycemia in diabetic mice. Transplantation. 2011; 91:11–20. [PubMed: 21452407]

7. Chandra V, Swetha G, Muthyala S, Jaiswal AK, Bellare JR, Nair PD, et al. Islet-like cell aggregates generated from human adipose tissue derived stem cells ameliorate experimental diabetes in mice. PLoS One. 2011; 6:e20615. [PubMed: 21687731]
8. Milanesi A, Lee JW, Li Z, Da Sacco S, Villani V, Cervantes V, et al. β-Cell regeneration mediated by human bone marrow mesenchymal stem cells. PLoS One. 2012; 7:e42177. [PubMed: 22879915]
9. Voltarelli JC, Couri CE, Stracieri AB, Oliveira MC, Moraes DA, Pieroni F, et al. Autologous nonmyeloablative hematopoietic stem cell transplantation in newly diagnosed type 1 diabetes mellitus. JAMA. 2007; 297:1568–76. [PubMed: 17426276]
10. Fiorina P, Voltarelli J, Zavazava N. Immunological applications of stem cells in type 1 diabetes. Endocr Rev. 2011; 32:725–54. [PubMed: 21862682]
11. Hu J, Yu X, Wang Z, Wang F, Wang L, Gao H, et al. Long term effects of the implantation of Wharton's jelly-derived mesenchymal stem cells from the umbilical cord for newly-onset type 1 diabetes mellitus. Endocr J. 2013; 60:347–57. [PubMed: 23154532]
12. Li Y, Zhang R, Qiao H, Zhang H, Wang Y, Yuan H, et al. Generation of insulin producing cells from PDX-1 gene-modified human mesenchymal stem cells. J Cell Physiol. 2007; 211:36–44. [PubMed: 17226789]
13. Sun Y, Chen L, Hou XG, Hou WK, Dong JJ, Sun L, et al. Differentiation of bone marrow-derived mesenchymal stem cells from diabetic patients into insulin-producing cells in vitro. Chin Med J. 2007; 120:771–6. [PubMed: 17531117]
14. Hisanaga E, Park KY, Yamada S, Hashimoto H, Takeuchi T, Mori M, et al. A simple method to induce differentiation of murine bone marrow mesenchymal cells to insulin-producing cells using conophylline and betacellulin-delta4. Endocr J. 2008; 55:535–43. [PubMed: 18480554]
15. Milanesi A, Lee JW, Xu Q, Perin L, Yu JS. Differentiation of nestin-positive cells derived from bone marrow into pancreatic endocrine and ductal cells in vitro. J Endocrinol. 2011; 209:193–201. [PubMed: 21330336]
16. Lechner A, Yang YG, Blacken RA, Wang L, Nolan AL, Habener JF. No evidence for significant transdifferentiation of bone marrow into pancreatic beta-cells in vivo. Diabetes. 2004; 53:616–23. [PubMed: 14988245]
17. Taneera J, Rosengren A, Renstrom E, Nygren JM, Serup P, Rorsman P, et al. Failure of transplanted bone marrow cells to adopt a pancreatic beta-cell fate. Diabetes. 2006; 55:290–6. [PubMed: 16443759]
18. Gao X, Song L, Shen K, Wang H, Niu W, Qin X. Transplantation of bone marrow derived cells promotes pancreatic islet repair in diabetic mice. Biochem Biophys Res Commun. 2008; 371:132–7. [PubMed: 18420028]
19. Perin L, Sedrakyan S, Giuliani S, Da Sacco S, Carraro G, Shiri L, et al. Protective effect of human amniotic fluid stem cells in an immunodeficient mouse model of acute tubular necrosis. PLoS One. 2010; 5:e9357. [PubMed: 20195358]
20. Sedrakyan S, Da Sacco S, Milanesi A, Shiri L, Petrosyan A, Varizemova R, et al. Injection of amniotic fluid stem cells delays progression of renal fibrosis. J Am Soc Nephrol. 2012; 23:661–73. [PubMed: 22302195]
21. Carraro G, Perin L, Sedrakyan S, Giuliani S, Tiozzo C, Lee J, et al. Human amniotic fluid stem cells can integrate and differentiate into epithelial lung lineages. Stem Cells. 2008; 11:2902–11. [PubMed: 18719226]
22. Buckley S, Shi W, Carraro G, Sedrakyan S, Da Sacco S, Driscoll BA, et al. The milieu of damaged alveolar epithelial type 2 cells stimulates alveolar wound repair by endogenous and exogenous progenitors. Am J Respir Cell Mol Biol. 2011; 45:1212. [PubMed: 21700959]
23. Garcia O, Carraro G, Turcatel G, Hall M, Sedrakyan S, Roche T, et al. Amniotic fluid stem cells inhibit the progression of bleomycin-induced pulmonary fibrosis via CCL2 modulation in bronchoalveolar lavage. Plos One. 2013; 8:e71679. [PubMed: 23967234]
24. Chun SY, Mack DL, Moorefield E, Oh SH, Kwon TG, Pettenati MJ, et al. Pdx1 and controlled culture conditions induced differentiation of human amniotic fluid-derived stem cells to insulin-producing clusters. J Tissue Eng Regen Med. 2012 Epub ahead of print.
25. Hay N. Akt isoforms and glucose homeostasis: the leptin connection. Trends Endocrinol Metab. 2011; 22:66–73. [PubMed: 20947368]

26. Komatsu M, Ruoslahti E. R-Ras is a global regulator of vascular regeneration that suppresses intimal hyperplasia and tumor angiogenesis. Nat Med. 2005; 11:1346–50. [PubMed: 16286923]
27. Dor Y, Brown J, Martinez OI, Melton DA. Adult pancreatic beta-cells are formed by self-duplication rather than stem-cell differentiation. Nature. 2004; 429:41–6. [PubMed: 15129273]
28. Nir T, Melton DA, Dor Y. Recovery from diabetes in mice by beta cell regeneration. J Clin Invest. 2007; 117:2553–61. [PubMed: 17786244]
29. Halban PA. Cellular sources of new pancreatic beta cells and therapeutic implications for regenerative medicine. Nat Cell Biol. 2004; 6:1021–5. [PubMed: 15516994]
30. Bonner-Weir S, Weir GC. New sources of pancreatic beta-cells. Nat Biotechnol. 2005; 23:857–61. [PubMed: 16003374]
31. Xu X, D'Hoker J, Stange G, Bonne S, De Leu N, Xiao X, et al. Beta cells can be generated from endogenous progenitors in injured adult mouse pancreas. Cell. 2008; 132:197–207. [PubMed: 18243096]
32. Bollini S, Cheung KK, Riegler J, Dong X, Smart N, Ghionzoli M, et al. Amniotic fluid stem cells are cardioprotective following acute myocardial infarction. J Stem Cells Dev. 2011; 20:1985–94.
33. Fayard E, Xue G, Parcellier A, Bozulic L, Hemmings BA. Protein kinase B (PKB/Akt), a key mediator of the PI3K signaling pathway. Curr Top Microbiol Immunol. 2010; 346:31–56. [PubMed: 20517722]
34. Chang F, Lee JT, Navolanic PM, Steelman LS, Shelton JG, Blalock WL, et al. Involvement of PI3K/Akt pathway in cell cycle progression, apoptosis, and neoplastic transformation: a target for cancer chemotherapy. Leukemia. 2003; 17:590–603. [PubMed: 12646949]
35. Heit JJ, Karnik SK, Kim SK. Intrinsic regulators of pancreatic beta-cell proliferation. Annu Rev Cell Dev Biol. 2006; 22:311–38. [PubMed: 16824015]
36. Bernal-Mizrachi E, Wen W, Stahlhut S, Welling CM, Permutt MA. Islet /3 cell expression of constitutively active Akt1/PKBa induces striking hypertrophy, hyperplasia, and hyperinsulinemia. J Clin Invest. 2001; 108:1631–8. [PubMed: 11733558]
37. Chen J, Somanath PR, Razorenova O, Chen WS, Hay N, Bornstein P, et al. Akt1 regulates pathological angiogenesis, vascular maturation and permeability in vivo. Nat Med. 2005; 11:1188–96. [PubMed: 16227992]
38. Somanath PR, Chen J, Byzova TV. Akt1 is necessary for the vascular maturation and angiogenesis during cutaneous wound healing. Angiogenesis. 2008; 11:277–88. [PubMed: 18415691]
39. Doble BW, Woodgett JR. GSK-3: tricks of the trade for a multi-tasking kinase. J Cell Sci. 2003; 116(Pt 7):1175–86. [PubMed: 12615961]
40. Liu Y, Tanabe K, Baronnier D, Patel S, Woodgett J, Cras-Meneur C, et al. Conditional ablation of Gsk-3/3 in islet beta cells results in expanded mass and resistance to fat feeding-induced diabetes in mice. Diabetologia. 2010; 53:2600–10. [PubMed: 20821187]
41. Grimes CA, Jope RS. The multifaceted roles of glycogen synthase kinase 3beta in cellular signaling. Prog Neurobiol. 2001; 65:391–426. [PubMed: 11527574]
42. Beurel E, Jope RS. The paradoxical pro- and anti-apoptotic actions of GSK3 in the intrinsic and extrinsic apoptosis signaling pathways. Prog Neurobiol. 2006; 79:173–89. [PubMed: 16935409]
43. Johansson M, Mattsson G, Andersson A, Jansson L, Carlsson PO. Islet endothelial cells and pancreatic beta-cell proliferation: studies in vitro and during pregnancy in adult rats. Endocrinology. 2006; 147:2315–24. [PubMed: 16439446]
44. Nikolova G, Jabs N, Konstantinova I, Domogatskaya A, Tryggvason K, Sorokin L, et al. The vascular basement membrane: a niche for insulin gene expression and beta cell proliferation. Dev Cell. 2006; 10:397–405. [PubMed: 16516842]
45. Lai Y, Schneider D, Kidszun A, Hauck-Schmalenberger I, Breier G, Brandhorst D, et al. Vascular endothelial growth factor increases functional beta-cell mass by improvement of angiogenesis of isolated human and murine pancreatic islets. Transplantation. 2005; 79:1530–6. [PubMed: 15940042]
46. Zhang W, Liu HT. MAPK signal pathways in the regulation of cell proliferation in mammalian cells. Cell Res. 2002; 12:9–18. [PubMed: 11942415]

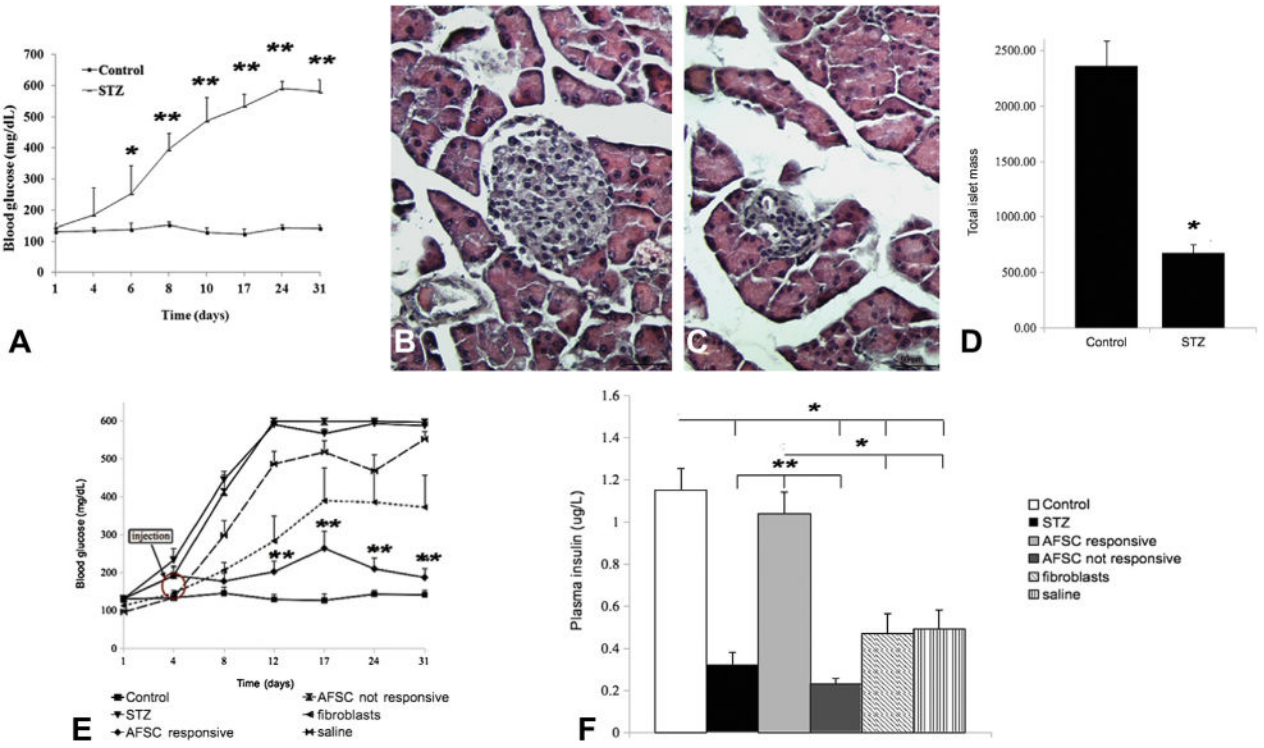

Figure 1.

Disease establishment and physiological response to AFSC injection: Establishment of the disease model. Mice receiving multiple low doses of STZ (50 mg/kg for 3 days) developed significant hyperglycemia by experimental day 8. Blood glucose levels remained sustained (600 mg/dL) up to 4 weeks after drug treatment, in contrast to that observed for the healthy control mice that maintained normoglycemia <200 mg/dL (A). STZ-treated mice showed strong islet mass reduction compared with healthy control mice, as revealed by hematoxylin and eosin staining (B,C). Quantification of total islet mass confirmed significant reduction of endocrine pancreatic tissue in diabetic mice 4 weeks after treatment (D). The physiological response of STZ-treated mice to AFSC transplantation was evaluated by detection of blood glucose levels for 4 weeks after AFSC injection and plasma insulin. AFSC-responsive mice displayed normoglycemic average value (<200 mg/dL) 4 weeks after cell injection, similar to that in healthy control mice and significantly lower than that observed in STZ-treated mice (~600 mg/dL). Both fibroblast and saline injections did not prevent development of hyperglycemia, with values ~400 mg/dL and ~550 mg/dL, respectively. A group of AFSC-injected mice did not respond to cell treatment (E, arrow: injected cells). Plasma insulin was quantified 4 weeks after cell treatment. AFSC-responsive mice presented a significantly higher level of circulating insulin compared with AFSC–non-responsive, STZ-treated and fibroblast-injected and saline-injected mice, which all conversely presented significantly reduced amounts of plasma insulin compared with the healthy control group (F). Magnification × 200. Scale bar =50 μm. *$P < 0.05$, **$P < 0.01$.

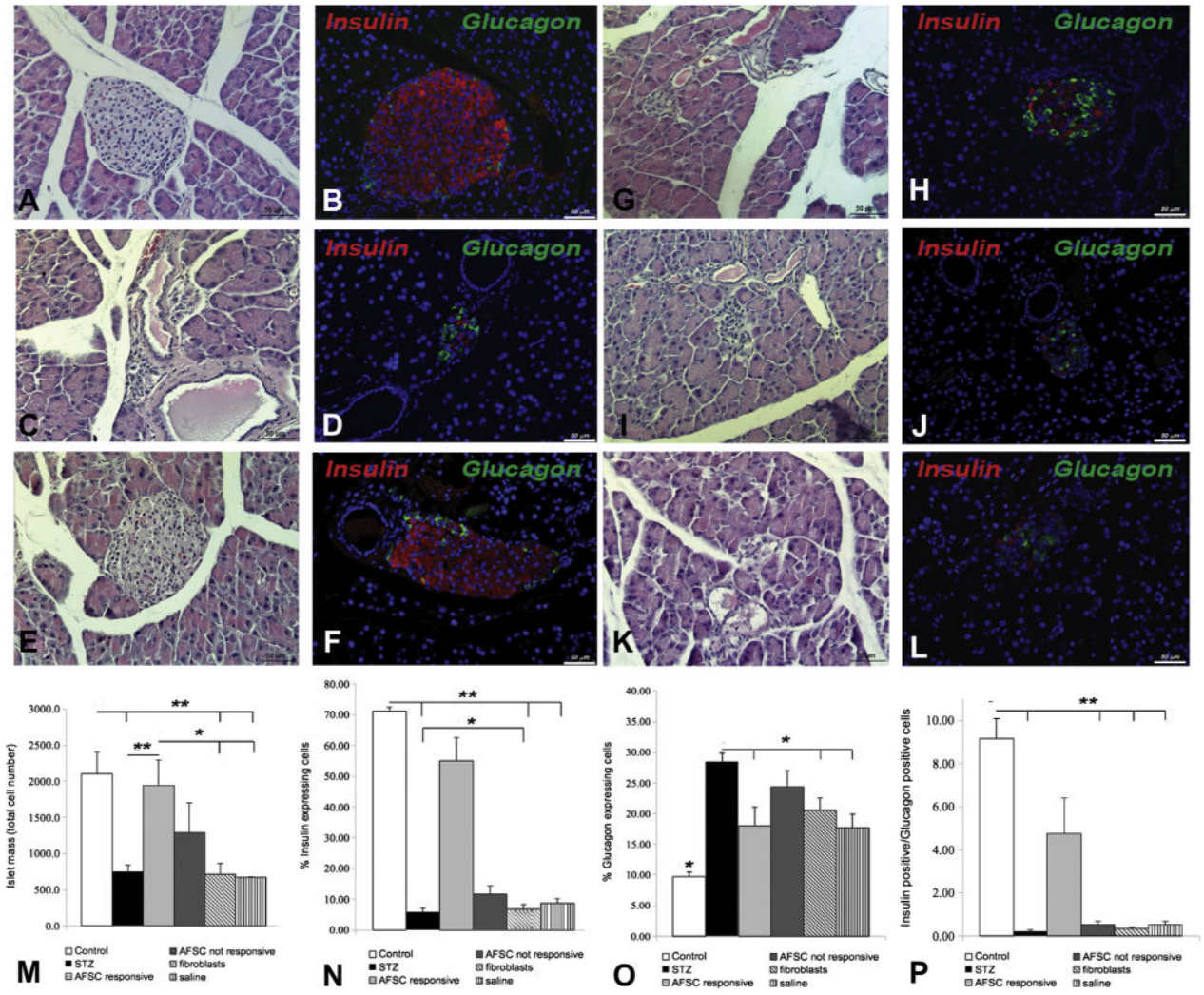

Figure 2.

Preservation of islet mass and insulin/glucagon expression 4 weeks post injection: Immunohistochemical and hematoxylin and eosin analysis of pancreata from different mouse groups: healthy control (A,B), STZ-treated (C,D), AFSC-responsive (E,F), AFSC non-responsive (G,H), fibroblast-injected (I,J) and saline-injected (K,L). hematoxylin and eosin staining (left column) and immunofluorescence double staining (right column) of insulin (red) and glucagon (green) 4 weeks after AFSC injection are shown. The preservation of islet mass in AFSC-responsive mice (E) compared with STZ-treated mice (C), AFSC–non-responsive mice (G), fibroblast-injected mice (I) and saline-injected mice (K) is notable. Morphological distribution of hormone-expressing cells was conserved in AFSC-responsive mice (F), showing a pattern similar to that observed in the healthy control mice (B). In contrast, STZ-treated mice (D), AFSC–non-responsive mice (H), fibroblast-injected mice (J) and saline-injected mice (L) showed a strong reduction of insulin-expressing cells and general disruption of islet architecture and cells distribution. Quantification of islet mass (M) and hormone-expressing cells (N,O) among different groups confirmed that AFSC-responsive mice have a significantly higher amount of islet

cell mass and insulin-expressing β-cells than do STZ-treated mice, AFSC–non-responsive mice, fibroblast-injected mice and saline-injected mice. All treatment groups presented a significant increase of glucagon-expressing α-cells compared with the healthy group. The ratio of insulin-positive cells versus glucagon-positive cells was quantified, confirming preservation of hormone-expressing cell ratios in AFSC-responsive mice compared with the other reference groups which all showed a significantly reduced ratio compared with healthy control mice (P). Magnification ×200. Scale bar = 50 μm. *$P < 0.05$, **$P < 0.01$.

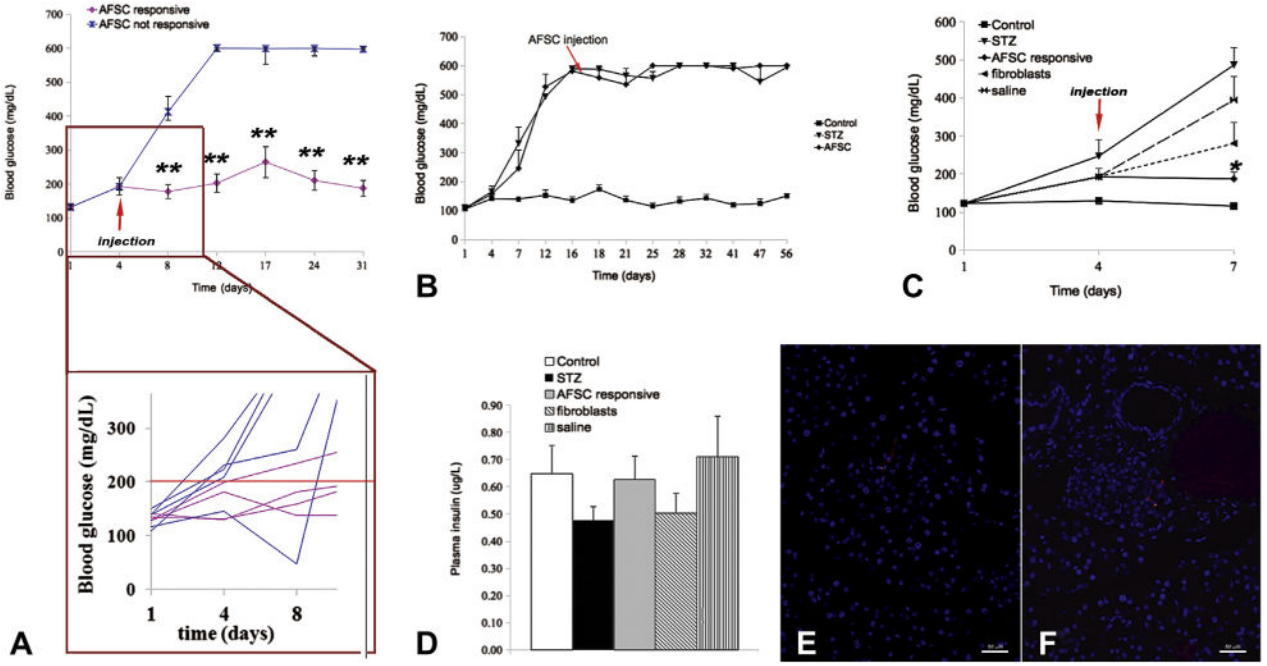

Figure 3.

Level of glucose at the time of cell injection correlated with response to AFSC treatment. (A) Blood glucose levels of mice at the time of AFSC injection (experimental day 4). It is evident that mice responding to AFSC treatment had regular blood glucose values at the moment of cell injection (≤200 mg/dL). Among the non-responsive mice, only one had glycemia ≤200 mg/dL at the time of cell injection but showed a generalized irregular trend, becoming severely hypoglycemic after cell injection before reaching definitive hyperglycemia. (B) Injection of AFSC at a later time point (14 days after STZ treatment) did not correct hyperglycemia, confirming that rescue is unlikely when hyperglycemia is already established and the acute phase of damage has occurred. AFSC injection was repeated for short-term result (72 h after injection). After STZ treatment, mice were AFSC-, fibroblast- or saline-injected and monitored for blood glucose (C) and plasma insulin (D) in the short term. AFSC-responsive mice showed normoglycemia, with significantly reduced levels compared with STZ-treated mice. Both fibroblast-injected and saline-injected mice presented glucose values slightly lower than STZ-treated mice, even though not statistically different and still above the threshold that defines hyperglycemia (250 mg/dL). (E,F) Detection of AFSC by CM-Dil labeling 72 h after injection. AFSC were homing in both exocrine (E) and endocrine (F) tissue. Magnification ×200. Scale bar = 50 μm. *$P < 0.05$, **$P < 0.01$ (arrow indicates injected cells).

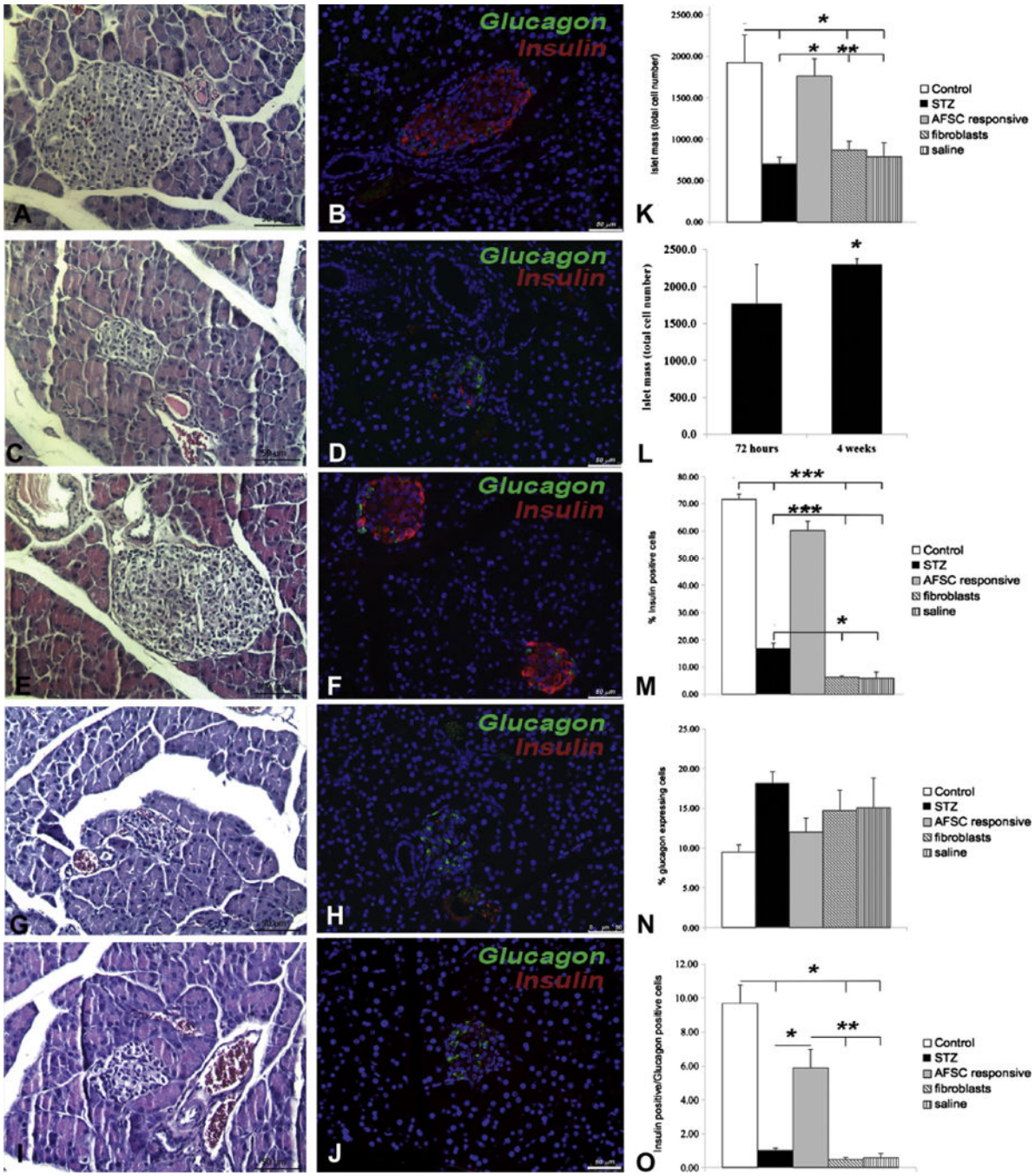

Figure 4.

Preservation of islet mass and insulin/glucagon expression 72 h after injection. Immunohistochemical analysis by hematoxylin and eosin staining (A,C,E,G,I) and immunofluorescence double staining for insulin and glucagon (B,D,F,H,J) show preservation of islet morphology and hormone expression in AFSC-injected mice (E,F), similar to that of healthy control mice (A,B). Conversely, STZ-treated mice (C,D), fibroblast-injected mice (G,H) and saline-injected mice (I,J) mice presented shrinkage of islet mass and modified hormone expression. Quantification of islet mass (K) revealed

significant preservation of endocrine mass in AFSC-responsive mice; analysis at 72 h and 4 weeks after cell transplantation also revealed a significant increase in total islet mass throughout experimental time (L). Levels of insulin expression were significantly preserved in AFSC-responsive mice, supporting previous data (M). Although glucagon expression did not show significant differences among experimental groups (N), the ratio of insulin-positive versus glucagon-positive cells was significantly preserved in AFSC-responsive mice (O). Magnification ×200. Scale bar = 50 μm. *$P < 0.05$, **$P < 0.01$, ***$P < 0.001$.

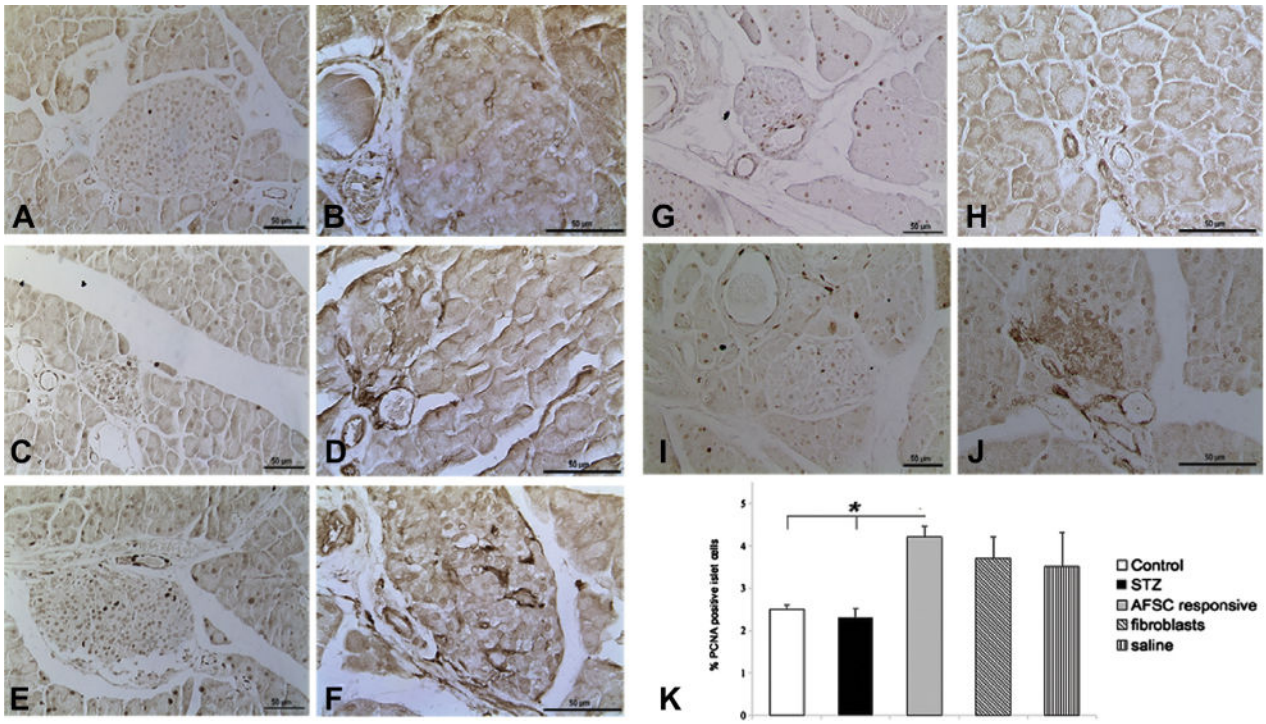

Figure 5.

Intra-islet proliferation and VEGF-A expression 72 h after injection. Cell proliferation within the islets of the different experimental groups was evaluated on tissue sections at 72 h after injection by immunostaining of PCNA and VEGF-A (A–J). Control (A) and STZ-treated (C) mice showed similar amounts of positive cells, whereas AFSC-responsive mice (E) revealed higher intra-islet expression of PCNA compared with the groups of fibroblast-injected mice (G) and saline-injected (I) mice. Immunoperoxidase staining analysis also showed stronger expression of VEGF-A in AFSC-responsive mice (F) compared with control mice (B), STZ-treated mice (D), fibroblast-injected mice (H) and saline-injected mice (J). Quantification of PCNA-positive cells within islets revealed a significant increase of proliferation in AFSC-responsive mice compared with healthy control mice and all other treatment groups (K). Magnification ×200 (PCNA), ×400 (VEGF-A). Scale bar = 50 μm. *$P < 0.05$.

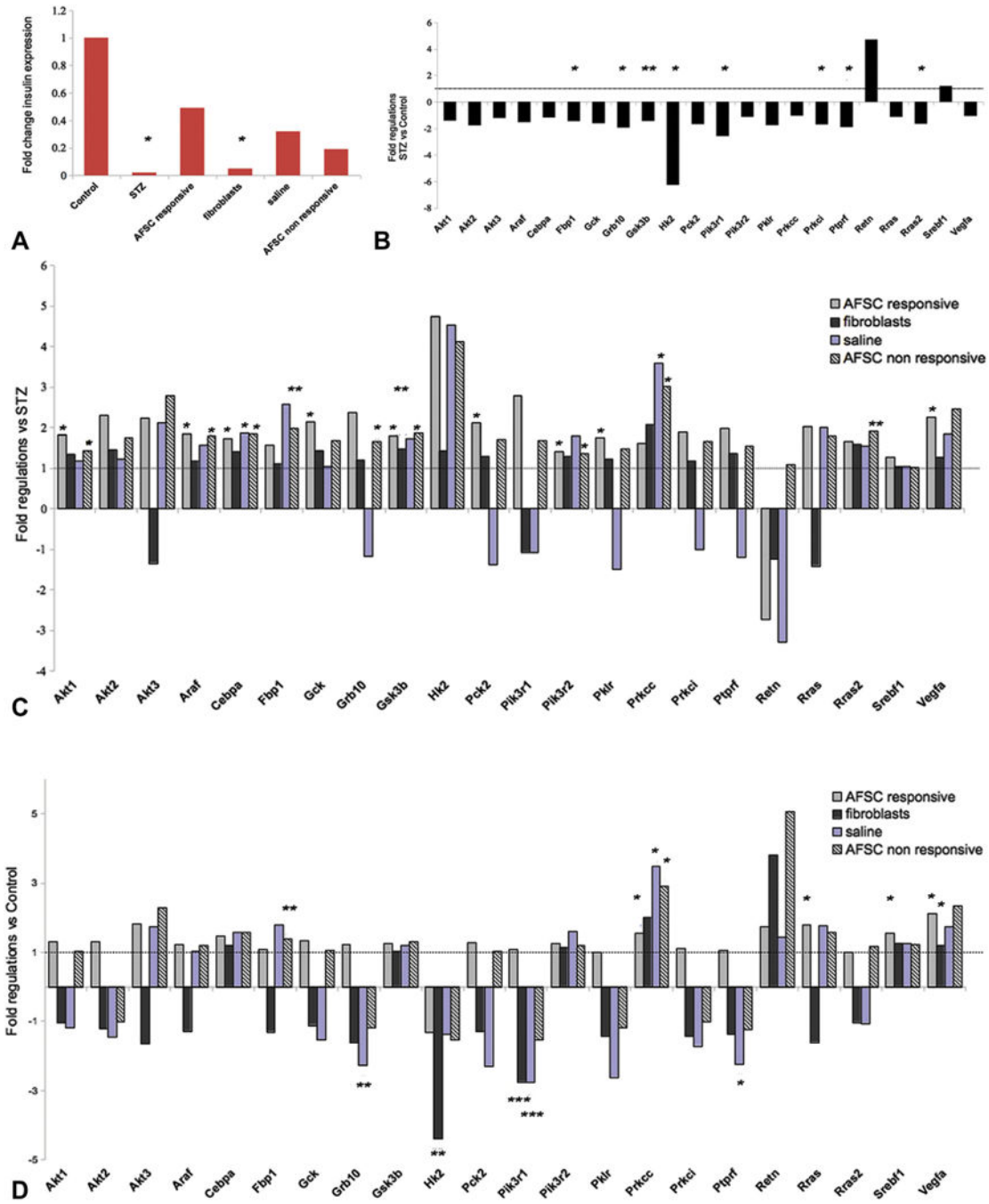

Figure 6.

Activation of the Pi3K pathway mediates protection and cell survival in AFSC-injected responsive mice: Insulin signaling pathway analysis by real-time PCR assay in the pancreatic tissue of all the experimental groups. (A) Fold changes relative to expression of the insulin gene in the different treatment groups and normalized to control. STZ-treated and fibroblast-injected mice presented significantly reduced amounts of insulin expression compared with the control group, and AFSC-responsive mice consistently displayed 24-fold higher expression compared with STZ-treated samples and generally higher expression than

all other injected groups. Gene expression analysis of STZ-treated mice versus control mice revealed a trend of downregulation for many genes, including genes required for glucose metabolism (*Fbp1*, *Hk2*) or involved in the insulin receptor and PI3K signaling pathways (*Grb10*, *Ptprf*, *Pik3r1* and *Prkc*) (B). Gene expression was evaluated for all injected groups (AFSC, responsive and non-responsive, fibroblast-injected and saline-injected) versus the STZ-treated group (C) and the control group (D) to determine differences or similarities, respectively, with our disease model and healthy animals. Statistically significant fold changes were considered. Upregulated genes in AFSC-responsive mice versus STZ-treated diabetic: *Gck*, *Pk2*, *Pklr* involved in glucose metabolism and *Akt1*, *Pik3r2*, *VEGF-A* of the *Pi3K* pathway, and other regulatory factors such as *Gsk3b*, *Araf* and *Cebpa*. **P* < 0.05, ***P* < 0.01, ****P* < 0.001.